REGULAR ARTICLE

blood advances

Anti–BAFF-R antibody VAY-736 demonstrates promising preclinical activity in CLL and enhances effectiveness of ibrutinib

Emily M. McWilliams,[1,2,*] Christopher R. Lucas,[3,*] Timothy Chen,[1,2,*] Bonnie K. Harrington,[2,4] Ronni Wasmuth,[2] Amanda Campbell,[1] Kerry A. Rogers,[2] Carolyn M. Cheney,[2] Xiaokui Mo,[5] Leslie A. Andritsos,[2] Farrukh T. Awan,[2] Jennifer Woyach,[2] William E. Carson III,[6] Jonathan Butchar,[2] Susheela Tridandapani,[2] Erin Hertlein,[2] Carlos E. Castro,[3] Natarajan Muthusamy,[2,†] and John C. Byrd[2,7,†]

[1]Biomedical Sciences Graduate Program, College of Medicine, [2]Division of Hematology, Department of Internal Medicine, College of Medicine and OSU Comprehensive Cancer Center, [3]Department of Mechanical and Aerospace Engineering, College of Engineering, [4]Department of Veterinary Biosciences, College of Veterinary and Comparative Medicine, [5]Center for Biostatistics, [6]Division of Surgical Oncology, Department of Surgery, College of Medicine and OSU Comprehensive Cancer Center, and [7]Division of Medicinal Chemistry, College of Pharmacy, The Ohio State University, Columbus, OH

Key Points

- The anti–BAFF-R antibody VAY-736 enhances antibody-dependent cellular cytotoxicity and blocks BAFF-mediated survival signaling in human CLL.
- VAY-736 enhances the in vivo activity of ibrutinib in a murine model of chronic lymphocytic leukemia through an ITAM-mediated mechanism.

The Bruton tyrosine kinase inhibitor (BTKi) ibrutinib has transformed chronic lymphocytic leukemia (CLL) therapy but requires continuous administration. These factors have spurred interest in combination treatments. Unlike with chemotherapy, CD20-directed antibody therapy has not improved the outcome of BTKi treatment. Whereas CD20 antigen density on CLL cells decreases during ibrutinib treatment, the B-cell activating factor (BAFF) and its receptor (BAFF-R) remain elevated. Furthermore, BAFF signaling via noncanonical NF-κB remains elevated with BTKi treatment. Blocking BAFF interaction with BAFF-R by using VAY-736, a humanized defucosylated engineered antibody directed against BAFF-R, antagonized BAFF-mediated apoptosis protection and signaling at the population and single-cell levels in CLL cells. Furthermore, VAY-736 showed superior antibody-dependent cellular cytotoxicity compared with CD20- and CD52-directed antibodies used in CLL. VAY-736 exhibited in vivo activity as a monotherapy and, when combined with ibrutinib, produced prolonged survival compared with either therapy alone. The in vivo activity of VAY-736 is dependent upon immunoreceptor tyrosine–based activation motif (ITAM)–mediated activation of effector cells as shown by using an ITAM-deficient mouse model. Collectively, our findings support targeting the BAFF signaling pathway with VAY-736 to more effectively treat CLL as a single agent and in combination with ibrutinib.

Introduction

Chronic lymphocytic leukemia (CLL) is the most prevalent form of adult leukemia. Palliative chemotherapy was the treatment mainstay of the past, with no study reporting improvement in overall survival (OS). Rituximab (RTX) revolutionized CLL therapy due to its ability to improve OS when combined with chemotherapy.[1-3] The success of RTX prompted efforts to improve CD20 antibody therapy by altering the binding site or modifying the innate immune cell–binding site (Fc region). Obinutuzumab (OBN) binds to a different site on CD20, mediates direct apoptosis, and is glycoengineered with a defucosylated Fc region to increase innate immune cell binding and antibody-dependent cellular cytotoxicity (ADCC).[4,5] A phase 3 trial found that OBN is more effective than RTX.[6]

As data on chemoimmunotherapy matured, agents targeting B-cell receptor signaling emerged that greatly changed the landscape of CLL therapy. Most prominent was ibrutinib, an irreversible inhibitor of Bruton tyrosine kinase (BTK).[7,8] The success of ibrutinib in both relapsed and refractory CLL was

Submitted 4 September 2018; accepted 2 January 2019. DOI 10.1182/bloodadvances.2018025684.

*E.M.M., C.R.L., and T.C. contributed equally to this study.

†N.M. and J.C.B. contributed equally to this study as joint senior authors.

For original data, please contact the corresponding authors at raj.muthusamy@osumc.edu or john.byrd@osumc.edu.

The full-text version of this article contains a data supplement.

dramatic, with 90% to 95% of patients responding and disease progression mostly in a subset of high-risk individuals.[9,10] As an initial therapy, ibrutinib has been even more successful, with responses in virtually all patients, prolonged remissions, and improvement in OS. Two initial phase 2 trials with ibrutinib for which 5-year or greater follow-up exists found that ~90% of patients remain in remission, a finding not matched by any chemoimmunotherapy regimen.[11,12] Although ibrutinib therapy has been transformative in treating CLL, it does have limitations, including absence of complete remission, thereby necessitating continuous therapy. In addition, adverse events prevent some patients from taking ibrutinib long term, and development of resistance occurs in a subset of patients.[13-15] Unfortunately, the addition of CD20 antibody to ibrutinib has not improved the outcome of patients with CLL, as was observed with chemotherapy.[16,17]

One reason that RTX does not improve the efficacy of BTK inhibitors is that CD20 expression decreases during ibrutinib therapy.[18] In addition, ibrutinib inhibits interleukin-2–inducible T-cell kinase, which is required for natural killer (NK) cell ADCC.[19] Given the previous success with combining antibody therapeutic agents with chemotherapy in CLL, we continue to search for viable alternative targets to CD20.

One such tumor surface protein that we hypothesized might be amenable to targeting in CLL is the B-cell activating factor (BAFF)-receptor (BAFF-R). BAFF is a member of the tumor necrosis factor (TNF) superfamily that supports normal B-cell development and proliferation.[20,21] BAFF-R engagement activates pro-survival activity in B cells by exclusively binding BAFF with high affinity[22-24] and driving antiapoptotic gene transcription of Bcl-2 family members via NF-κB–inducible kinase–mediated alternative NF-κB signaling.[25-27] The CLL microenvironment, which is composed in part by stromal endothelial cells and nurse-like cells, supports survival of the malignant CLL B cells by producing a proliferation-inducing ligand (APRIL) and BAFF.[28-30] One study found that the Eμ-TCL1 mouse model of CLL[31] developed disease earlier and had shorter survival when crossed with stromal cell–expressing BAFF transgenic mice, suggesting that BAFF signaling is a driving factor in disease progression.[32] BAFF expression by stromal cells has also been shown in mantle cell lymphoma and CLL to mediate chemotherapy resistance,[33,34] but, to date, the influence of ibrutinib on this signaling pathway has not been examined. The present study identifies that the BAFF signaling pathway, driving primarily the alternative NF-κB signaling pathway, is not antagonized by ibrutinib and that expression of BAFF remains high during treatment with this agent. Given the inability of ibrutinib to antagonize alternative NF-κB signaling in vivo, we hypothesized that antagonizing this signaling pathway with the therapeutic antibody VAY-736,[35] previously called B-1239, might improve the efficacy of ibrutinib treatment. Herein, we use the glycoengineered defucosylated Fc-domain BAFF-R–blocking antibody VAY-736 to confirm this hypothesis.

Materials and methods

Human sample preparation and cell culture

Blood samples were obtained from patients with CLL[36] or healthy donors following written, informed consent under an institutional review board–approved protocol according to the Declaration of Helsinki. Peripheral blood mononuclear cells were separated by Ficoll density gradient centrifugation (Ficoll-Paque Plus; GE Healthcare, Chicago, IL) and isolated via negative selection for B cells or NK cells with RosetteSep (STEMCELL Technologies, Vancouver, BC, Canada). Cells were cultured at 37°C with 5% carbon dioxide atmospheric conditions in RPMI 1640 (Thermo Fisher Scientific, Waltham, MA) supplemented with 10% heat-inactivated fetal bovine serum (MilliporeSigma, Burlington, MA), 2 mM L-glutamine (Thermo Fisher Scientific), and 56 U/mL penicillin with 56 μg/mL streptomycin (Thermo Fisher Scientific). The OSU-CLL cell line has been described previously.[37] Monocytes were positively selected by using the Magnetic Activated Cell Sorting System (Miltenyi Biotec, Cambridge, MA) and differentiated into monocyte-derived macrophages by culture with monocyte-colony stimulating factor (R&D Systems, Minneapolis, MN) for 7 days.

Reagents

RTX, ofatumumab (OFA), OBN, alemtuzumab, and trastuzumab (TRA) were purchased from the OSU pharmacy. Novartis (East Hanover, NJ) provided the following: VAY-736[35] (previously called B-1239), VAY-736 labeled-PE, immunoglobulin G subclass 1 isotype labeled-PE, VAY-736 Fc-variant N297, VAY-736 labeled-Dylight633, immunoglobulin G subclass 1 isotype labeled-Dylight633, and recombinant human BAFF (PeproTech, Rocky Hill, NJ). Ibrutinib for in vivo studies was sourced from Acorn PharmaTech, LLC (Redwood City, CA).

Flow cytometry and reagents

Beckman Coulter FC500 and Gallios Flow Cytometers were used (Brea, CA), and data were analyzed by using Kaluza software (Beckman Coulter). BAFF-R expression and antibody-binding assays were conducted with fluorochrome-labeled monoclonal antibodies purchased from Becton Dickinson (Franklin Lakes, NJ). Antibodies include mouse anti-human CD19-PE (SJ25C1), CD5-FITC (L17F12), and CD56-APC (NCAM16.2) and antibodies generated in rat against mouse CD19 (1D3), CD5-FITC (53-7.3), and CD45-APC (30-F11). The BD Pharmingen anti–BAFF-R–PE (11C1) with wild-type Fc domain binding was compared with VAY-736–PE to observe VAY-736 engaging cells via its variable region or by its glycoengineered defucosylated Fc-domain. Gating was verified with appropriately matched isotype controls and/or with Fluorescence Minus One. To compare binding of antibodies to cells, delta mean fluorescence intensity (ΔMFI) was calculated: ΔMFI = (MFI experimental) – (MFI isotype); negative MFI is reported as 0.0.

Functional assays

Viability assays were conducted by flow cytometry using fluorescein isothiocyanate conjugated annexin V and propidium iodide in 1X Annexin V–binding buffer (BD Biosciences, Franklin Lakes, NJ) as previously described.[5] ADCC assays were performed by using a standard 4-hour ^{51}Cr-release assay. Antibody-dependent cellular phagocytosis (ADCP) assays were performed by using published methods.[5] TNF-α, interferon-γ (IFN-γ), and BAFF levels were determined in triplicate by using an enzyme-linked immunosorbent assay (R&D Systems) per the manufacturer's directions. Isolation of nuclear and cytoplasmic lysates was performed by using the NE-PER Kit (Thermo Fisher Scientific). Immunoblot experiments were performed by using established methods.[5] The following antibodies were used for detection: p100/p52 (MilliporeSigma), actin (I-19; Santa Cruz Biotechnology, Dallas, TX), and Lamin B (Santa Cruz Biotechnology). After antibody incubations, proteins

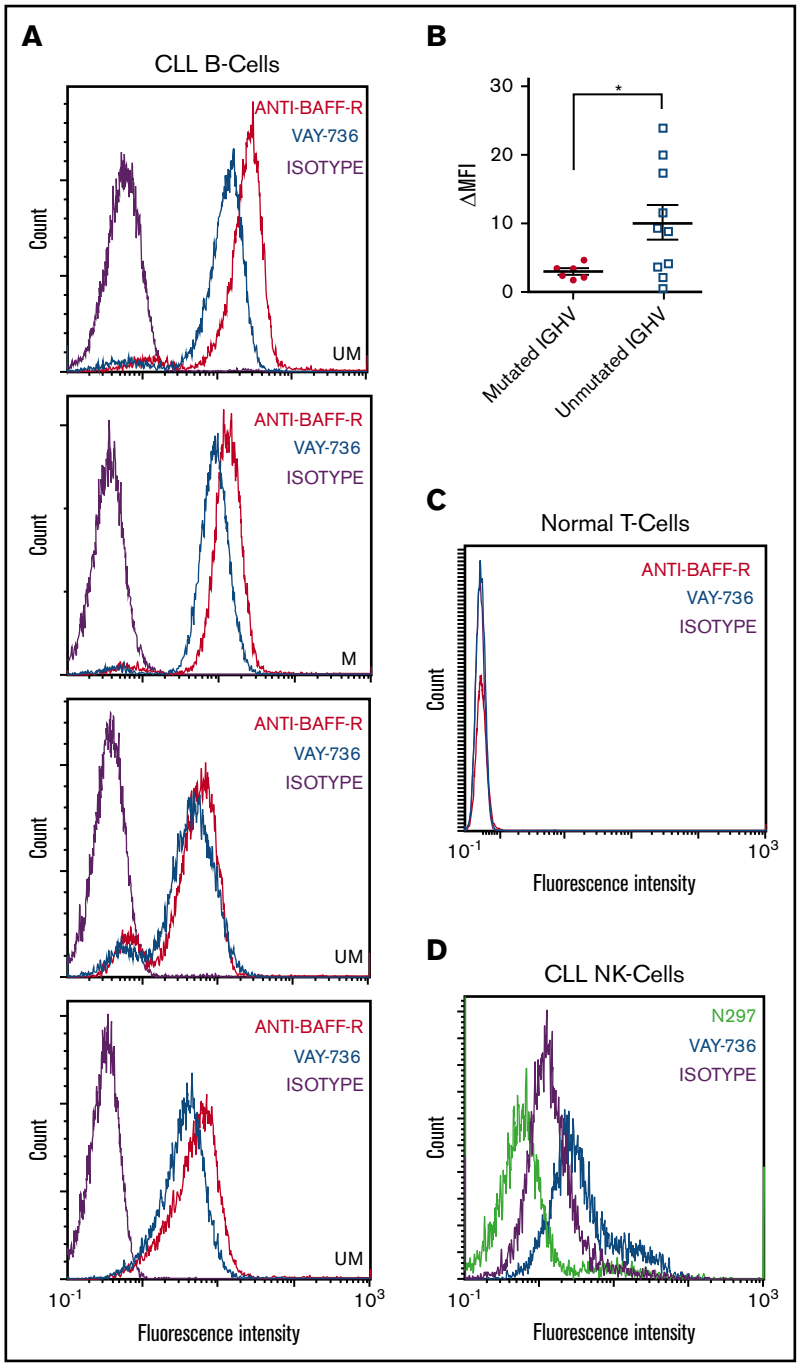

Figure 1. VAY-736 engages surface molecules on CLL B cells and NK cells. Flow cytometry analysis of VAY-736 binding profile on different cell subsets enriched from primary CLL or healthy donor blood. Peripheral blood mononuclear cells are stained with fluorochrome-conjugated VAY-736, anti–BAFF-R (11C1), isotype control, or VAY-736 variant with null Fc binding (N297). (A) Four CLL B-cell samples, IGHV mutated (M) or unmutated (UM) ($CD45^+$, $CD19^+$, and $CD5^+$) stained with VAY-736 (blue) and anti–BAFF-R (11C1) (red) compared with isotype control (purple). (B) Patients ΔMFI stratified according to IGHV mutational status ($P < .05$ mutated vs unmutated; mutated, n = 6; unmutated, n = 10; 2-sample Student *t* test). (C) Representative flow cytometry analysis of VAY-736 or anti–BAFF-R binding to healthy T cells ($CD45^+$, $CD3^+$, and $CD19^-$; n = 10). (D) Representative flow cytometry analysis of VAY-736 and N297 binding to CLL NK-cells ($CD45^+$, $CD56^+$, and $CD3^-$; n = 8). *$P < .05$.

were detected with chemiluminescent substrate (Thermo Fisher Scientific) and quantified by using the ChemiDoc system with AlphaView software (Protein Simple, San Jose, CA). Single-cell fluorescence microscopy methodology is outlined in the supplemental Materials and Methods.

Animal studies

All animal procedures were performed in accordance with federal and Institutional Animal Care and Use Committee requirements. Eμ-TCL1 transgenic mice (C57BL/6 background) have been described elsewhere.[31,38] Other strains used include C.B17 severe combined immunodeficiency (SCID) mice and NOTAM mice lacking FcR signaling potential.[39] Details regarding the experimental design of the in vivo studies can be found in the supplemental Materials and methods.

Histopathological analysis

One of the authors (B.K.H.) performed the pathologic analysis of hematoxylin and eosin–stained sections. Sections of spleen and bone marrow were fixed in 10% neutral buffered formalin, paraffin embedded, sectioned at 3 μM onto glass slides, and stained with hematoxylin and eosin.

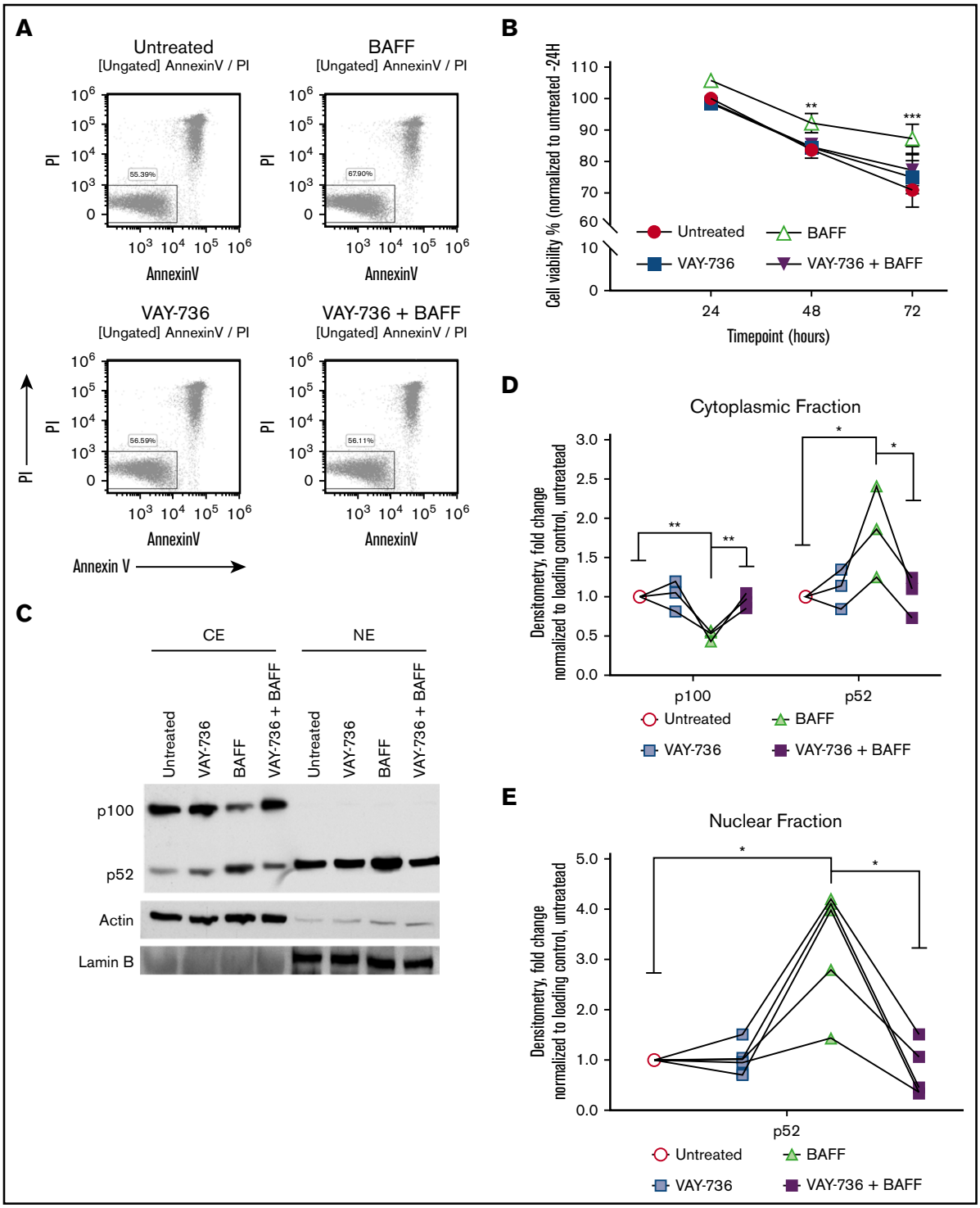

Figure 2. BAFF-mediated survival is blocked by VAY-736 treatment of CLL B cells. (A) Representative annexin V/propidium iodide (PI) flow cytometry analysis of a CLL patient B-cell viability at 72 hours. (B) Time course comparison of primary CLL cells' viability at 24, 48, and 72 hours treated with BAFF (500 ng/mL), VAY-736, or cells pretreated with VAY-736 subsequently stimulated with BAFF ($P < .001$: 72 hours, BAFF vs untreated; $P < .01$: 48 hours, VAY-736 + BAFF vs BAFF). Inhibitory effect of VAY-736 at each time point was tested by interaction contrast (BAFF + VAY-736 subtracting BAFF vs VAY-736 subtracting untreated; 72 hours, $P < .01$). Data were analyzed by using a mixed effect model, and Holm's method was used to adjust multiplicity (n = 21 patients). (C-E) Western blot analysis of p100 and p52 protein levels in primary CLL patient B cells. Treatments were soluble BAFF (500 ng/mL) for 16 hours with or without pretreatment with VAY-736 (10 μg/mL). Activation of alternative NF-κB was determined by separate cytoplasmic (CE) and nuclear (NE) protein fractions, loading controls actin (cytoplasmic), and Lamin B (nuclear). Quantification of p100 or p52 protein by densitometry analysis was normalized to loading control and then to the untreated condition ($P < .01$: cytoplasmic p100, VAY-736 + BAFF vs BAFF; $P < .05$: p52 cytoplasmic and nuclear levels, BAFF vs untreated, VAY-736 + BAFF vs BAFF; n = 5 CLL patients, 3 independent experiments). *$P < .05$, **$P < .01$, and ***$P < .001$.

Statistical analysis

Because many of the measurements used samples from the same patients, mixed effect models were used for analysis to take into consideration the dependency of these observations. Survival studies are illustrated by using Kaplan-Meier plots, and survival probabilities of treatment groups were compared by using log-rank tests. Trend analysis was used to compare the rates of leukemic cell depletion among groups.[40] The Bonferroni stepdown procedure[41] was used to control the family-wise error rate at 0.05. Statistical significance was determined by using SAS version 9.4 (SAS Institute, Inc., Cary, NC); $*P < .05$, $**P < .01$, and $***P < .001$.

Results

Specificity of VAY-736 to BAFF-R on B cells and FcγR on NK cells

BAFF-R expression has been shown to be present on normal B cells and CLL cells.[24,42] VAY-736 binds to CLL cells (Figure 1A) with increased variability on unmutated IGHV versus mutated IGHV patients (Figure 1B). As expected, VAY-736 lacks detectable T-cell binding (Figure 1C), supporting the high B-cell–specific expression of BAFF-R. We identified VAY-736 binding to NK cells, a cell type not known to express BAFF-R (Figure 1D), and hypothesized that this binding was by virtue of its glycoengineered Fc domain specifically modified to exhibit higher affinity for FcγRIIIa (CD16a). Indeed, the VAY-736 variant control (N297) with mutated Fc domain that abolishes FcγR binding failed to bind to NK cells. These collective findings and no detectable BAFF-R messenger RNA in NK cells (data not shown) support the theory that VAY-736 is binding to NK cells via FcγRIIIa.

VAY-736 decreases viability of BAFF-treated CLL cells

Spontaneous apoptosis of CLL cells occurs ex vivo,[30,43,44] and BAFF-R engagement via BAFF treatment significantly diminishes this action (Figure 2A, representative analysis at 72 hours; Figure 2B, summary of 21 patients). Although VAY-736 does not promote direct CLL cytotoxicity, pretreatment with VAY-736 blocked BAFF-mediated protection of CLL cells ($P < .01$), consistent with previous reports that VAY-736 engagement with the BAFF-R blocks BAFF binding to cells.[35] BAFF-R engagement mediates pro-survival activity in normal B cells by driving antiapoptotic gene transcription via an NF-κB–inducible kinase–mediated alternative NF-κB pathway.[26] This action occurs via p100 partial degradation to its subunit p52, nuclear translocation of p52/RelB, and binding of p52/RelB to NF-κB DNA binding motifs.[25] Similar signaling occurs in CLL with BAFF treatment, whereas pretreatment of CLL cells with VAY-736 before BAFF prevented the BAFF-R–dependent p100 cytoplasmic degradation and inhibited the BAFF-R–induced increase of p52 levels in the cytoplasmic and nuclear fractions ($P < .01$) (Figure 2C, representative blot; Figure 2D-E).

Although these findings reveal that VAY-736 is able to antagonize the BAFF-R signaling at the bulk cellular level, the level of variability in NF-κB signaling at the single-cell level remained unclear. Evaluating an intracellular signaling response at the single-cell level not only allows for increased measurement sensitivity but also a more representative and precise evaluation of the entire cell population because tumor populations are inherently heterogeneous.[45,46] Single-cell analysis also allows for a direct comparison of equal cell numbers across treatment groups. To confirm that BAFF activated NF-κB at the single-cell level and to test the ability of VAY-736 to block BAFF activation of NF-κB, we used the OSU-CLL cell line transduced with an expression vector containing tandem repeat elements for NF-κB binding upstream of the green fluorescent protein (*GFP*) coding sequence. This action allows us to measure transcriptional response of both canonical and noncanonical NF-κB in terms of relative fluorescence units of GFP expression. Single-cell fluorescent microscopy analysis confirmed that VAY-736 pretreatment inhibited BAFF-induced NF-κB–driven GFP expression ($P < .001$) (Figure 3A, representative figure; Figure 3B). To monitor NF-κB activity in real time and matching in vivo conditions, time-lapse live cell imaging experiments were performed over a 14-hour time course. BAFF stimulation resulted in a robust time-dependent increase in NF-κB activity, and pretreatment with VAY-736 substantially reduced the level of NF-κB activity with soluble BAFF addition ($n = 48$ single OSU-CLL cell traces) (Figure 3C-D). Importantly, BAFF/BAFF-R engagement in the presence of RTX revealed an elevation in NF-κB activity (supplemental Figure 1A), suggesting that the observed effect with VAY-736 was mediated by specifically blocking BAFF-R and not by virtue of antibody binding to cells. Together, these findings confirm that BAFF engagement of the BAFF-R triggered NF-κB activation pro-survival signaling at the single-cell level in OSU-CLL cells, an effect that was blocked by VAY-736.

Conserved BAFF-mediated NF-κB activity in ibrutinib-treated CLL patient cells

Shinners et al[47] showed that BTK couples BAFF-R and B-cell receptor to NF-κB using mice with the xid phenotype and BTK deletion. In $BTK^{-/-}$ mice, BAFF-mediated activation of alternative NF-κB signaling was reduced due to low p100 levels. After showing that serum BAFF levels remain elevated in patients with CLL at 2 and 3 months during ibrutinib therapy (supplemental Figure 2A), we sought to determine if this treatment antagonized BAFF signaling. CLL cells were incubated with ibrutinib or control for 1 hour followed by BAFF stimulation. BAFF induced p100 processing and p52 nuclear translocation in ibrutinib-treated cells, whereas VAY-736 pretreatment prevented BAFF-mediated p100 processing and p52 nuclear translocation ($P < .01$) (Figure 4A, representative figure; Figure 4B). To extend this finding, single-cell fluorescence microscopy analysis was used in OSU-CLL cells as described earlier. BAFF-mediated NF-κB signaling was not compromised in ibrutinib-treated OSU-CLL cells ($P < .001$) (Figure 4C, representative figure; Figure 4D). In contrast, VAY-736 blocked NF-κB reporter activity in BAFF-stimulated cells ($P < .001$). In this same model, ibrutinib decreased NF-κB reporter activity in anti–immunoglobulin M stimulated control conditions compared with vehicle conditions ($P < .05$, $n = 46$ single cells/condition) (supplemental Figure 1B). This finding validates BAFF activation of alternative NF-κB signaling in ibrutinib-treated cells through the BAFF-R.

VAY-736 showed enhanced ADCC and cytokine production by CLL NK cells

We compared ADCC mediated by VAY-736 vs other clinically relevant antibody therapeutic agents for CLL. VAY-736 at 0.1 μg/mL mediated potent ADCC against CLL B-cell targets (mean relative cytotoxicity, 76.28%), which was significantly greater than that of OFA (49.76%), RTX (35.36%), and trastuzumab

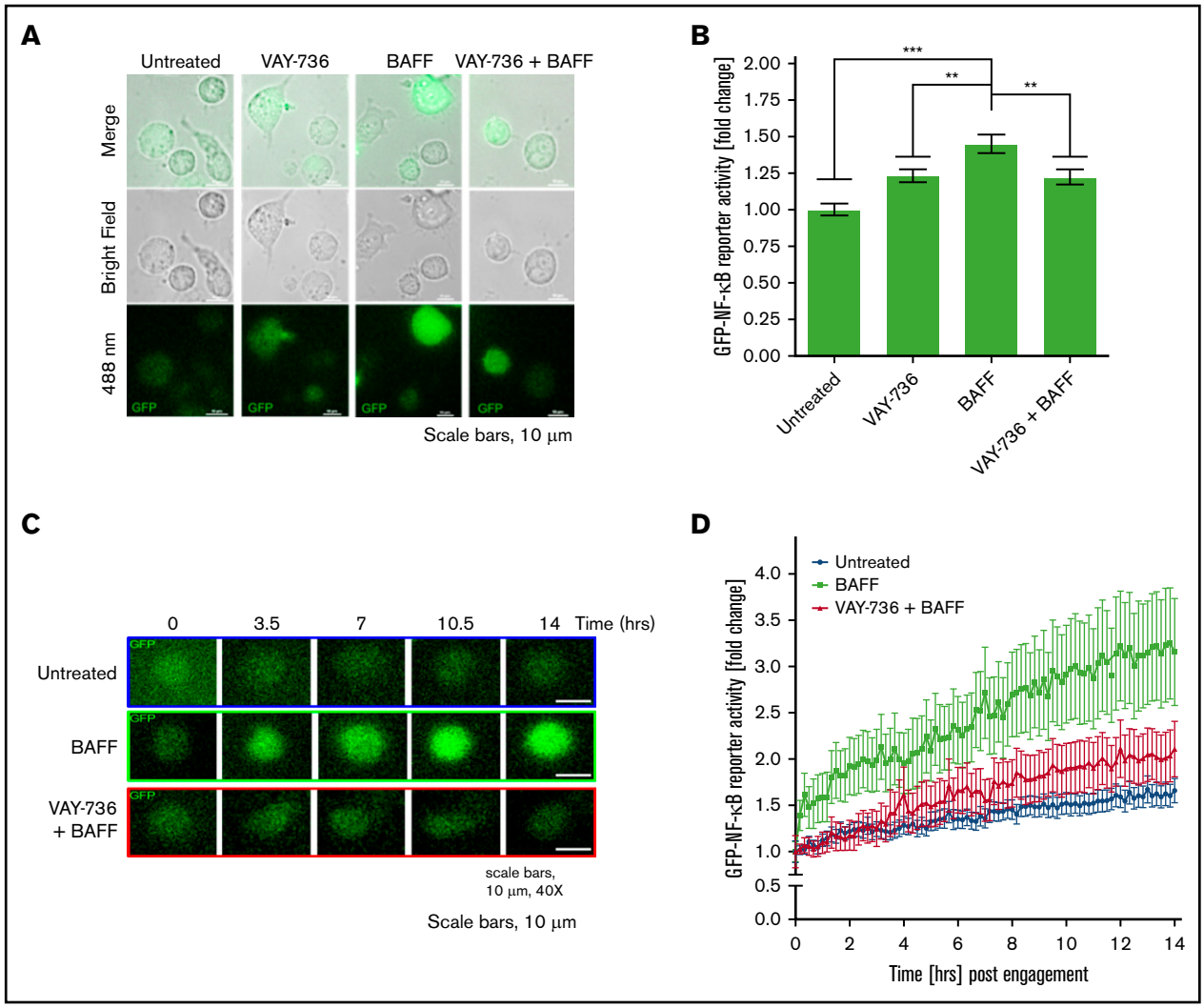

Figure 3. VAY-736 blocks BAFF-mediated activation of NF-κB at the single-cell level. (A) OSU-CLL cells were transduced with Cignal–GFP–NF-κB Lenti-viral reporter construct (Qiagen, Hilden, Germany). Cells were treated with VAY-736 with or without 16-hour BAFF stimulation (500 ng/mL). GFP–NF-κB activity (488 nm) was measured via fluorescent microscopy. Analysis of GFP–NF-κB activity was performed by using NIS-Elements software (Nikon Instruments, Tokyo, Japan). A representative image from 5 independent experiments is shown. (B) Data are expressed as relative florescence unit (RFU) mean fold change ± standard error of the mean (SEM) relative to untreated control. Mean background fluorescence was subtracted from single OSU-CLL cells that were transfected with the negative control construct. The data represent 5 independent experiments. A one-way analysis of variance followed by Bonferroni post hoc analysis was performed to determine statistical significance between groups (n = 435 single cells). (C) Representative 14-hour time lapse of single OSU-CLL cell GFP–NF-κB activity. GFP–NF-κB levels in VAY-736–treated cells were comparable to untreated control cells (data not shown). (D) Compiled 14-hour time lapse data of single cells monitored for GFP–NF-κB activity (488 nm) expressed as relative florescence unit mean fold change ± SEM relative to untreated control (n = 48 single cells, >3 independent experiments) treated with BAFF (500 ng/mL), pretreatment of VAY-736 (10 μg/mL), or untreated. $^{**}P < .01$ and $^{***}P < .001$.

(22.50%) ($P < .001$) (Figure 5A). VAY-736 mediated superior NK-ADCC over glycoengineered CD20 antibody OBN at 0.1 μg/mL (76.28% vs 45.84%; $P < .0001$), down to concentrations of 0.0001 μg/mL (42.17% vs 3.77%; $P < .001$). At concentrations of 0.00001 μg/mL, anti-CD20 antibodies RTX, OFA, and OBN exhibited virtually no killing, whereas VAY-736 mediated 20.21% killing activity ($P < .002$; n = 7). These findings support that VAY-736 mediated potent and superior NK cell ADCC activity against CLL B cells compared with the CD20-directed antibodies RTX, OBN, and OFA.

The superior ADCC activity observed with VAY-736 to OBN was unexpected due to their similarly defucosylated Fc domains. Because cytolytic $CD56^{dim}$ $CD16^{+}$ NK cells secrete IFN-γ after activation, which promotes NK:target cell conjugation leading to increased target cell lysis,[48,49] we hypothesized that VAY-736–enhanced NK cell–mediated killing of targets was through increased IFN-γ release. IFN-γ production was significantly detected more in NK cells drugged with VAY-736 than with OBN at 10 μg/mL (1468.0 vs 490.3 pg/mL; $P < .05$, n = 3) (Figure 5B), suggesting that the ability of VAY-736 to induce NK IFN-γ release may partially explain the enhanced killing of CLL tumor cell targets.

To test the ability of VAY-736 to activate cytokine production of myeloid cells, we evaluated whether CLL patient monocytes or monocyte-derived macrophages (MDMs) could release TNF-α after culture with VAY-736. As shown in Figure 5C-D, monocytes and MDMs displayed increased levels of TNF-α cytokine release after

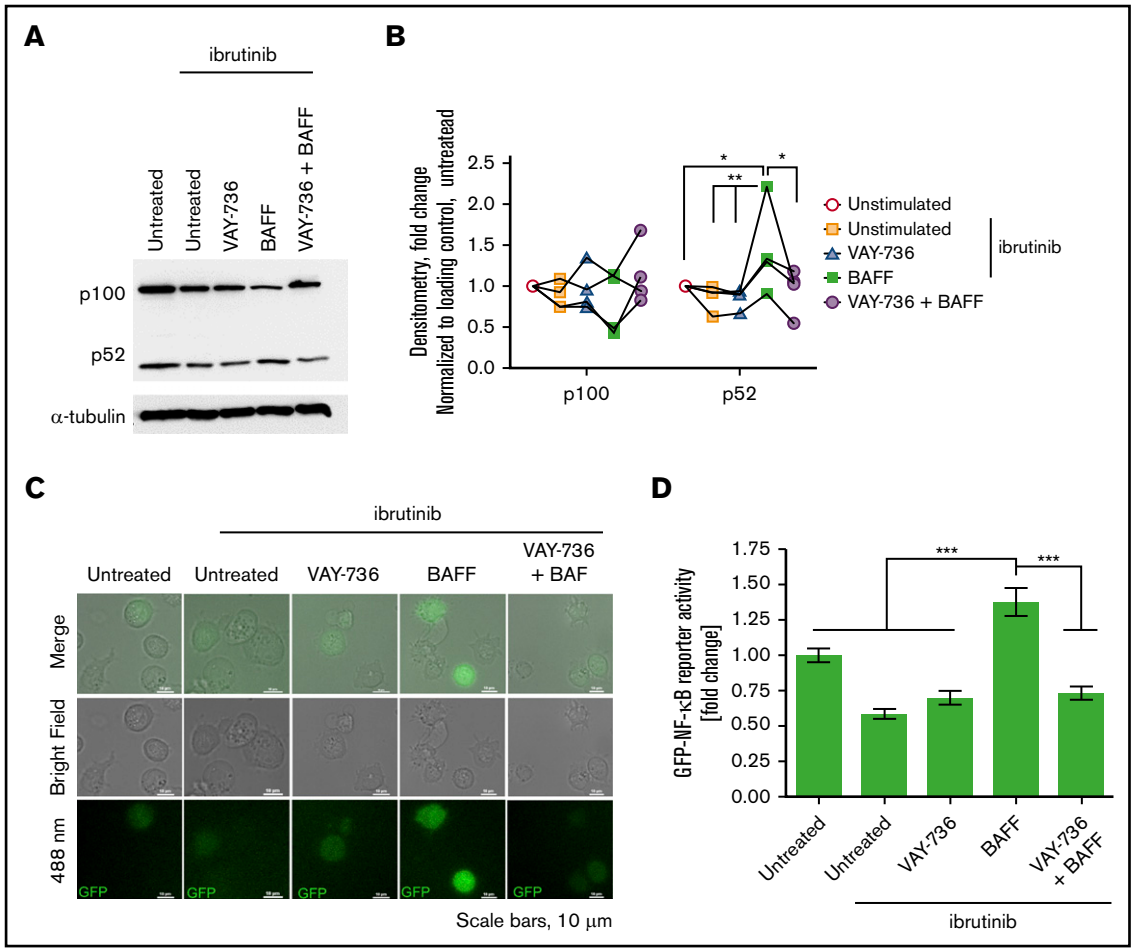

Figure 4. BAFF stimulates NF-κB signaling in CLL treated with ibrutinib. (A-B) Western blot and densitometry analysis of p100 and p52 protein levels in primary CLL patient B-cell cytoplasmic-enriched protein lysates. Treatments with ibrutinib (1 μM) or dimethyl sulfoxide (vehicle) control for 1 hour and washed out, and followed by 16 hours of vehicle, BAFF (500 ng/mL), VAY-736 (10 μg/mL), or VAY-736 + BAFF. (C-D) OSU-CLL cells transduced with Lenti–viral Cignal–GFP–NF-κB reporter were pretreated with ibrutinib (1 μM) or dimethyl sulfoxide vehicle control followed by treatments of BAFF (500 ng/mL), VAY-736 (10 μg/mL), or VAY-736 + BAFF. GFP–NF-κB activity was measured via fluorescent microscopy 14 hours posttreatment. A representative image is shown (n = 106 single cells, 3 independent experiments). Data are expressed as the mean RFU fold change ± SEM relative to the vehicle control. A one-way analysis of variance followed by Bonferroni post hoc analysis was performed to determine whether statistical significance existed between groups. *$P < .05$, **$P < .01$, and ***$P < .001$.

plate-bound antibody stimulation (VAY-736 vs no antibody: monocytes, $P < .01$; MDMs, $P < .01$ [n = 3]). VAY-736 triggered macrophage ADCP of CLL cells comparable to the antibody therapeutic agents RTX, OBN, and OFA that was significant over untreated conditions ($P < .05$; n = 3; Figure 5E). This finding is in agreement with previous reports showing similar ADCP levels between RTX and defucosylated CD20 antibody OBN-stimulated macrophages.[5]

VAY-736 increases in vivo survival in CLL mouse models

We confirm that VAY-736 binds to the $CD19^+$ $CD5^+$ cells of murine splenocytes derived from the Eμ-TCL1 CLL mouse model (Figure 6A). Eμ-TCL1 mice with active leukemia were treated once per week for 2 weeks with VAY-736 at the preclinical highest repeatable dose of 100 mg/kg (the no observable adverse effects level). Absolute counts and percentage of blood $CD5^+$ $CD19^+$ leukemic B cells were serially monitored over time. Blood B cells at pretreatment compared with 24 hours posttreatment (Figure 6B, representative example) revealed a significant reduction in circulating leukemic cells from 3.6×10^7 cells/mL to 2.7×10^6 cells/mL (Figure 6C), along with a decrease in the mean percentage of circulating leukemic lymphocytes (78.1% to 5.2%) (Figure 6D). These low leukemic counts were maintained up to 80 days posttreatment.

After verifying that VAY-736 was not cytotoxic to Eμ-TCL1 splenocytes in vitro (data not shown), we tested if VAY-736 could provide a survival advantage at a dose concentration lower than the no observable adverse effects level. Splenocytes from leukemic Eμ-TCL1 mice were transferred into SCID mice, and when leukemia was evident, mice were given VAY-736 (10 mg/kg) or control antibody once a week for 6 weeks. This treatment provided a survival advantage over vehicle control ($P < .05$) (Figure 6E). NOTAM mice express normal surface levels of FcRγ but are unable to signal due to mutations in the receptor's immunoreceptor tyrosine–based activation motif (ITAM), which primarily antagonizes ADCC function and allows us to interrogate NK-cell functions without deletion of Fc receptors or depletion of NK cells.[50] We

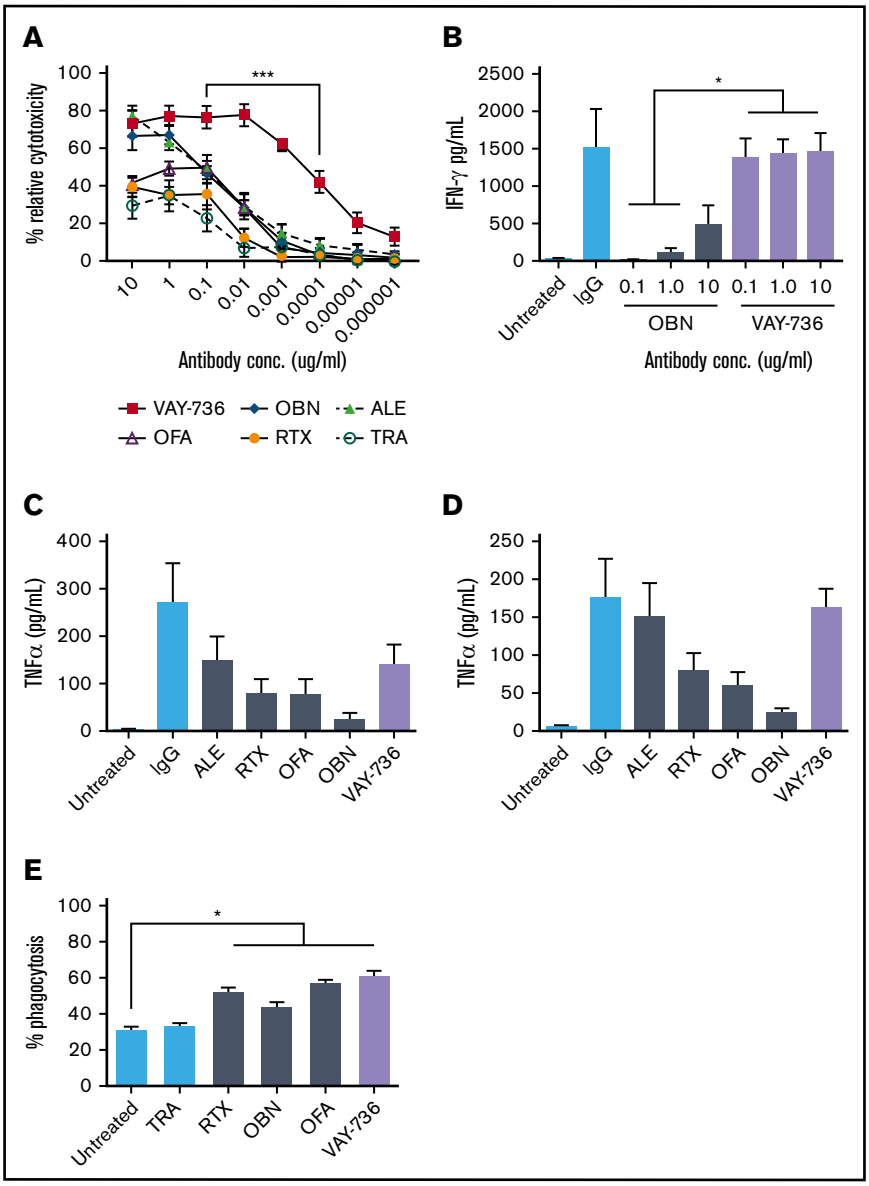

Figure 5. VAY-736 enhances ADCC and NK-cell activation. (A) ^{51}Cr release assays comparing ADCC mediated by VAY-736 with allogeneic normal donor NK cells and CLL target B cells ($P < .001$, n = 8 normal donor; n = 7 CLL). (B) Enzyme-linked immunosorbent assay data of IFN-γ release by NK cells incubated with plate-bound VAY-736 vs OBN at 10, 1.0, and 0.1 μg/mL; $P < .05$, n = 3 NKs, 2 separate experiments. (C-D) Enzyme-linked immunosorbent assay data comparing TNF-α release by monocytes (C) or MDMs (D) stimulated with plate-bound VAY-736, OBN, OFA, RTX, alemtuzumab (ALE), or immunoglobulin G (IgG) (not significant, n = 3). (E) MDMs were labeled with Claret, and CLL B cells were stained with PKH67. ADCP was observed by using flow cytometry and measuring the percentage of cells double-positive for Claret PKH67 ($P < .05$: untreated vs RTX, vs OBN, vs OFA, vs VAY-736; n = 3). *$P < .05$ and ***$P < .001$. TRA, trastuzumab.

injected NOTAM mice with splenocytes from a highly leukemic Eμ-TCL1 mouse to assess the requirement of ITAM function for in vivo efficacy of VAY-736. Unlike the rapid peripheral leukemia eradication seen in the Eμ-TCL1 SCID mouse model, the disease burden was comparable in VAY-736–treated vs vehicle-treated mice in the NOTAM mouse model with nonsignaling FcRγ (Figure 6F). Furthermore, no differences in leukemic burden were observed between vehicle-treated and VAY-736–treated mice in either the spleen or bone marrow at day 12 posttreatment (Figure 6G). These data support the importance of FcRγ receptor ITAM-dependent effector functions, including ADCC, in mediating the cytotoxic effects of VAY-736.

Combining VAY-736 and ibrutinib in vivo enhances efficacy and survival advantage

Because our findings thus far suggested potent ADCC activity with VAY-736, we hypothesized that the increased affinity for FcγRIIIa on NK cells could overcome ibrutinib-mediated NK-cell impairment. To address this theory, we adoptively transferred splenocytes from a leukemic Eμ-TCL1 mouse into SCID mice and randomly assigned them to vehicle, VAY-736, ibrutinib, or combination VAY-736 + ibrutinib treatment groups. Median survival of the VAY-736 + ibrutinib combination treatment group was 170 days (n = 9) and increased significantly compared with monotherapy alone (Figure 7A) (vs VAY-736 = 115 days, $P < .05$, n = 13; vs ibrutinib = 79 days, $P < 0.01$, n = 13). Tissues were harvested from recipient mice 6 weeks postenrollment and analyzed by histopathology to observe and evaluate leukemia infiltration in lymphoid organs (Figure 7B). Spleens from vehicle-treated or ibrutinib-treated mice were markedly enlarged compared with mice treated with VAY-736 or VAY-736 + ibrutinib. In addition, we detected expanded splenic white pulp caused by leukemic cells, which were visible as white foci in the enlarged spleens. Although ibrutinib slowed the rate of leukemia in the blood, addition of VAY-736 eliminated blood leukemia through week 10 (Figure 7C, WBC counts; Figure 7D, peripheral

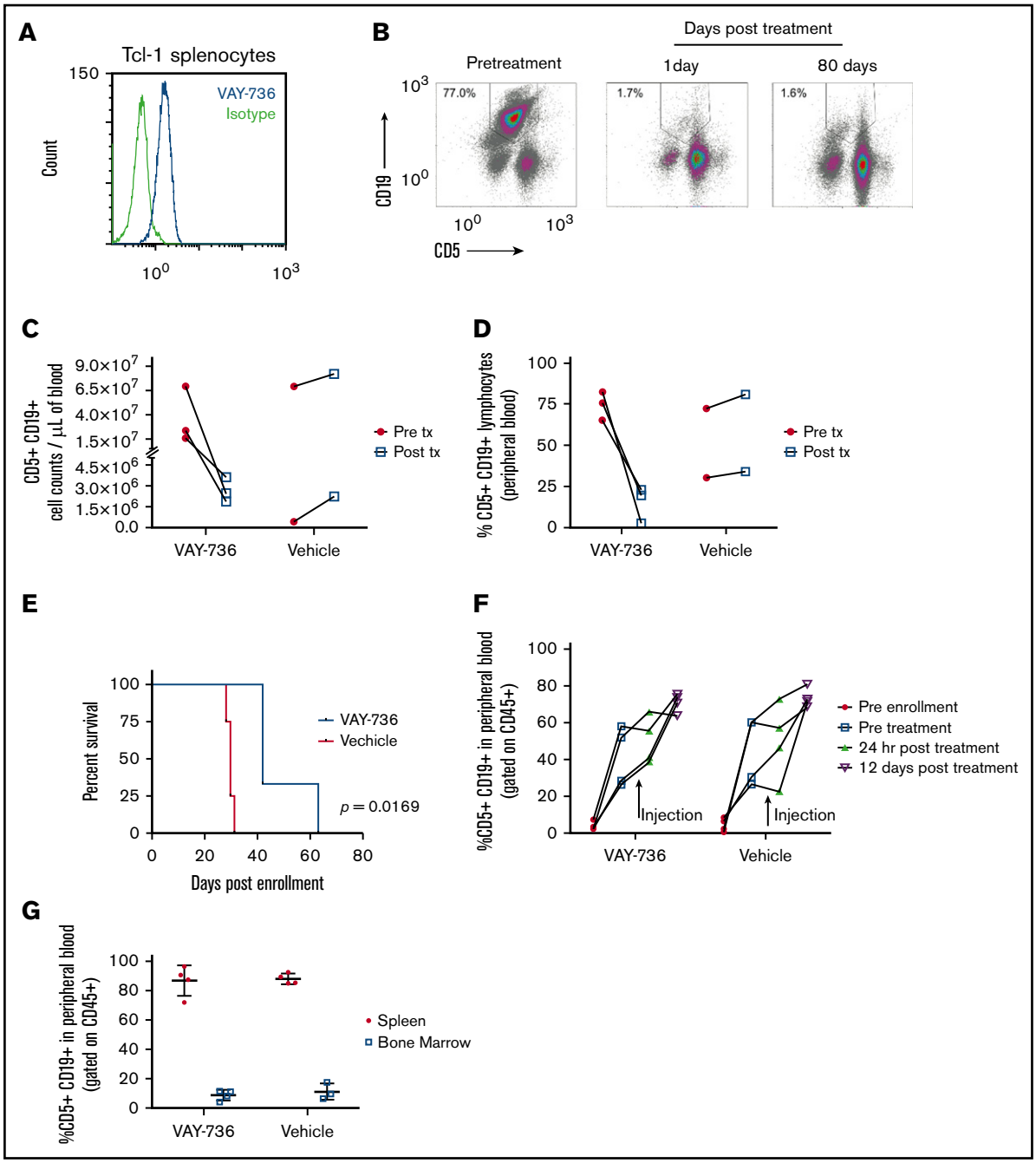

Figure 6. In vivo efficacy of VAY-736 in the Eμ-Tcl1 mouse model of CLL. (A) Histogram flow cytometry analysis of VAY-736 binding over isotype to $CD5^+$ $CD19^+$ double-positive Eμ-TCL1 mouse splenocytes. (B) Representative FACS of $CD5^+$ $CD19^+$ percent double-positive leukemia lymphocyte population in peripheral blood samples from a leukemia-burdened Eμ-TCL1 transgenic mouse. Mice were injected weekly for 2 weeks total with 100 mg/kg of VAY-736. Blood was collected 1 day after treatment and weekly. (C-D) Peripheral blood from Eμ-TCL1 mice were collected 24 hours before (Pre tx) and 24 hours after (Post tx) injection of VAY-736 at 100 mg/kg or phosphate-buffered saline (PBS) vehicle control, and $CD5^+$ $CD19^+$ double-positive leukemic cells were counted (C) and percentages were analyzed (D) by using flow cytometry. (E) Survival analysis of SCID mice engrafted with leukemia-burdened Eμ-TCL1 splenocytes from a single donor. SCID mice were enrolled in the study when $CD5^+$ $CD19^+$ percent lymphocytes from peripheral blood reached >20% within 9 weeks of engraftment. Mice received weekly injections of VAY-736 (10 mg/kg) or PBS vehicle control for 6 weeks ($P = .0169$: VAY-736; n = 3, vs vehicle, n = 4). (F) Eμ-TCL1 splenocytes from a highly leukemic burdened mouse were adoptively transferred into NOTAM mice. Peripheral leukemic percentages were monitored by using flow cytometry before engraftment, pretreatment, 24 hours posttreatment, and at 12 days posttreatment with either VAY-736 injection (10 mg/kg) or vehicle (PBS). (G) Mice from panel F were euthanized at day 12 posttreatment, and the leukemic burden of the spleen and bone marrow were analyzed according to percent $CD5^+$ $CD19^+$ by using flow cytometry.

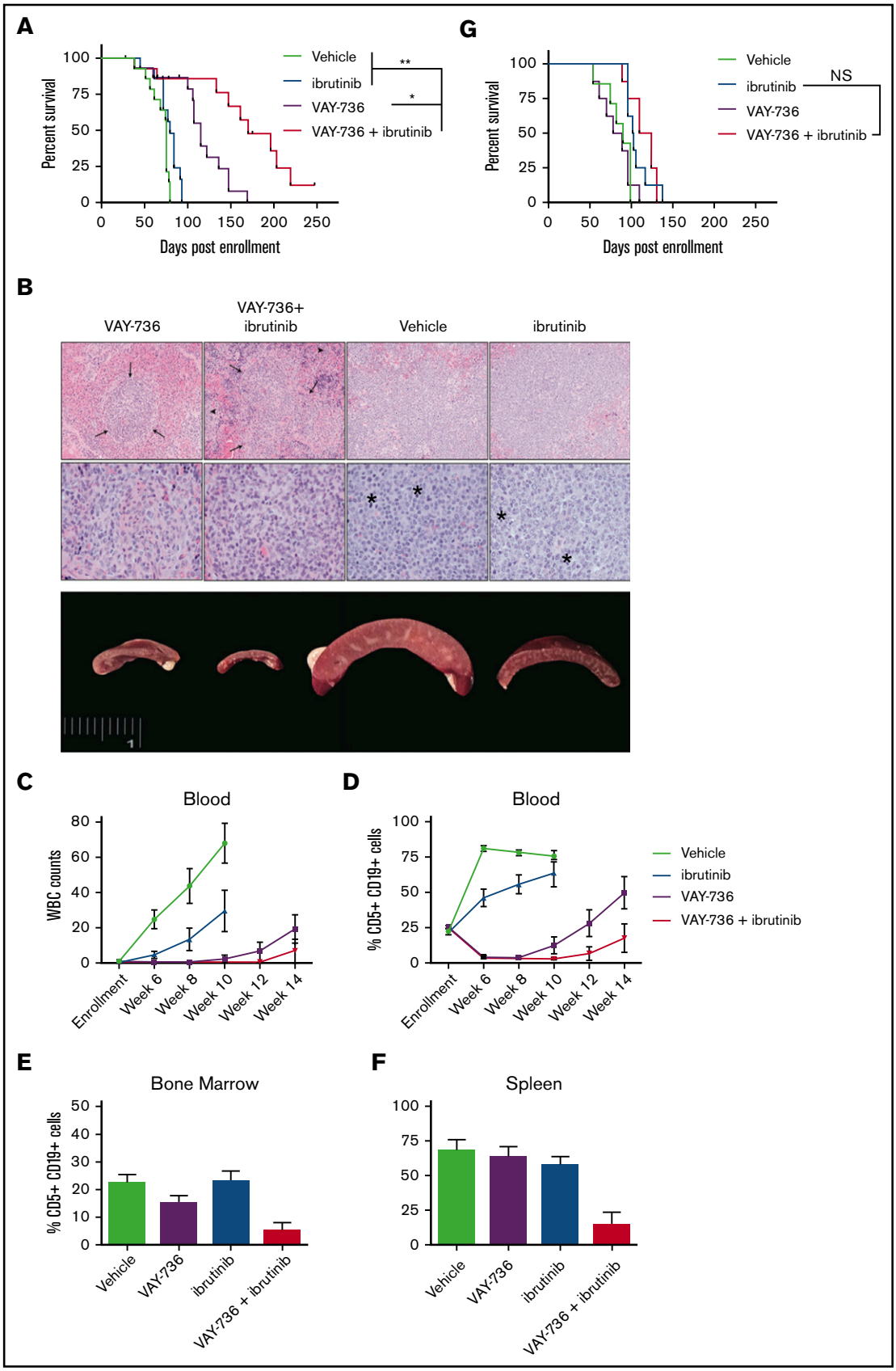
A
Percent survival
Days post enrollment
Vehicle
ibrutinib
VAY-736
VAY-736 + ibrutinib
**
*
G
NS
B
VAY-736
VAY-736+ ibrutinib
Vehicle
ibrutinib
C
Blood
WBC counts
Enrollment
Week 6
Week 8
Week 10
Week 12
Week 14
D
Blood
% CD5+ CD19+ cells
E
Bone Marrow
F
Spleen

Figure 7.

blood percent $CD5^+$ $CD19^+$). Postmortem analysis of mouse spleen and bone marrow revealed less disease burden in animals given VAY-736 + ibrutinib treatment compared with monotherapy with VAY-736 or ibrutinib (Figure 7E-F).

VAY-736 and ibrutinib in vivo activity is dependent on ITAM function

To determine if the added benefit of VAY-736 to ibrutinib was dependent on blocking of BAFF survival signaling or ITAM function, we repeated this combination strategy in the NOTAM mice. NOTAM mice were engrafted with Eμ-TCL1 leukemic cells, and mice were randomized according to the experimental design in Figure 7A. No added efficacy was shown when VAY-736 was added to ibrutinib in this model (Figure 7G), supporting the theory that the added benefit of ibrutinib + VAY-736 is due to the influence of Fcγ activation by ITAM-containing immune effector cells.

Discussion

The present study shows the novelty of targeting BAFF-R in CLL with the antibody therapeutic VAY-736. The defucosylated Fc-domain of VAY-736 engaged NK cells to deliver potent ADCC to CLL cells, even at very low concentrations, and the killing activity was superior to that of all other therapeutic antibodies currently available for CLL treatment. Similarly, VAY-736 enhanced IFN-γ production by CLL NK cells at concentrations where OBN was inactive. Innate immune cell activation of monocytes and macrophages was also superior or equal, as shown by proinflammatory cytokine release and ADCP. In addition to this potent therapeutic mechanism, in BAFF-stimulated cells, VAY-736 blocked NF-κB activation and reduced leukemic cell viability, offering a second potential therapeutic mechanism of killing. After identifying that BAFF signaling can activate downstream NF-κB signaling even in the presence of BTK inhibition, we hypothesized that this antibody could synergize with ibrutinib. This theory was corroborated by in vivo experiments in which combining VAY-736 and ibrutinib significantly improved survival and reduced disease burden in the Eμ-TCL1 leukemia model. Collectively, findings from this study provide justification for further clinical development of VAY-736 as a therapeutic agent in CLL and suggest that VAY-736 may be an ideal antibody for combination with ibrutinib as opposed to anti-CD20 antibodies.

A previous report showed that VAY-736 is highly effective at depleting human acute lymphoblastic leukemia cells in vitro and decreasing tumor burden in vivo, and found that VAY-736 binds to BAFF-R epitopes that are part of the BAFF ligand-binding site.[35] Herein, we extend this finding to CLL and show for the first time that ibrutinib does not block BAFF signaling in CLL cells. The activation of BAFF downstream signaling that was dependent on BTK has been previously reported in murine B cells by Shinners et al,[47] who showed that BTK deficiency reduced, but not abolished, BAFF induced alternative NF-κB signaling. Our observation that BAFF signaling can still be activated even in the context of BTK inhibition with ibrutinib is consistent with those findings and provides an alternative mechanism of BTK inhibitor resistance. The ability of VAY-736 to block BAFF-R on CLL cells is a novel concept for immunotherapy, as is our finding that in human CLL cells, antagonizing BTK signaling does not block NF-κB signaling by BAFF stimulation. Although most antibodies are designed to target a cell-specific marker, here we highlight the advantage in targeting a receptor that is both cell-specific and involved in survival signaling.

The full extent to which blocking BAFF or BAFF-R will contribute to CLL eradication remains unclear. In vitro, the presence of B-cell maturation antigen–Fc decoy receptors reduces the viability of CLL cells by binding up BAFF and APRIL; however, the BAFF-R–Fc decoy receptor was unable to reduce the viability of CLL cells.[30] In the viability assays reported here, BAFF protected CLL cells from spontaneous apoptosis, and anti–BAFF-R treatment with VAY-736 inhibited a BAFF-mediated boost in viability. This finding suggests that blocking BAFF's specific interaction with BAFF-R, not just quenching BAFF in the serum, is essential to block survival of CLL cells, and furthermore that BAFF/BAFF-R is a critical mechanism for mediating survival. VAY-736 is advantageous in its ability to both interfere with the BAFF/BAFF-R survival axis and to facilitate highly effective and rapid antibody-mediated clearance of target cells. An alternative BAFF-R antibody was also recently reported, with promising activity in drug-resistant human B-cell malignancies.[34]

To our surprise, despite the blocking ability of BAFF by VAY-736, which we hypothesized might contribute to improve efficacy of ibrutinib in vivo, the lack of ITAM function in immune effector cells in the NOTAM mouse removed any added benefit of VAY-736 efficacy in the Eμ-TCL1 adoptive transplant model of murine CLL. This finding suggests that ibrutinib enhancement of VAY-736 activity occurs through an ITAM function on NK cells. Given the enhanced activation and cytokine production of NK cells when exposed to VAY-736, we hypothesize that ibrutinib, by alternative target inhibition of interleukin-2–inducible T-cell kinase, may diminish activation-induced death of NK and other innate immune effector cells in vivo, as we have shown with NK cells and T cells ex vivo.[51] Future studies to elucidate this mechanism are ongoing in our laboratory. These studies elucidating 2 separate therapeutic mechanisms of VAY-736 in CLL provide strong support for the clinical development of VAY-736 in this disease. We have further

Figure 7. VAY-736 combines effectively with ibrutinib in vivo. Tumor-derived splenocytes from disease-burdened Eμ-TCL1 mice were engrafted into SCID mice. (A) Kaplan-Meier survival plot receiving weekly VAY-736 (10 mg/kg) retro-orbital injections, vehicle control injections, ibrutinib drinking water, or combination VAY-736 + ibrutinib, for up to 6 injections of VAY-736 or vehicle, and continuous ibrutinib drinking water provided through study. Leukemic death was confirmed upon death by fluorescence-activated cell sorting analysis of blood, spleen, and bone marrow $CD5^+$ $CD19^+$ percentage of lymphocytes (VAY-736 + ibrutinib vs ibrutinib, $P < .0001$; VAY-736 + ibrutinib vs VAY-736, $P = .06$; n = 14 per group). Adjustments for multiple comparisons for the log-rank test were used for data analysis. *$P < .05$ and **$P < .01$. (B) After 6 weeks, 2 animals per group were euthanized and samples sent for histopathology analysis. Splenic white pulp expanded by leukemia cells is visible as white foci in the enlarged spleens. Splenic white pulp areas (arrows) and red pulp (arrow heads) are infiltrated and expanded by leukemia cells in all specimens. Top row: photomicrographs at low-power magnification to show level of infiltration (magnification ×20; hematoxylin and eosin stain). Middle row: high-power magnification to show cellular detail (magnification ×60; hematoxylin and eosin stain). Mitotic figures are indicated with an asterisk. Bottom row: gross anatomy images of spleens. White blood cell (WBC) counts from blood smears (C) and $CD5^+$ $CD19^+$ percent circulating lymphocytes (D) were observed weekly for leukemia progression. (E-F) At death, spleen and bone marrow were analyzed by fluorescence-activated cell sorting for percent lymphocytes $CD5^+$ $CD19^+$. (G) Kaplan-Meier survival plot of a repeated experiment described in panel A except with engraftment into NOTAM mice lacking functional FcRγ (VAY-736 + ibrutinib vs ibrutinib, $P = .4921$; VAY-736 vs vehicle, $P = .7453$; n = 7 to 8 per group). NS, not significant.

shown that both these mechanisms are active in the presence of ibrutinib, and these data provide the preclinical rationale for a recently initiated phase 1 clinical trial of VAY-736 in combination with ibrutinib (#NCT03400176).

Acknowledgments

This work was supported by the National Institutes of Health, National Cancer Institute (R35 CA197734, R01 CA177292, and R01 CA183444), the Leukemia and Lymphoma Society, the D. Warren Brown Foundation, Four Winds Foundation, the Sullivan Chronic Lymphocytic Leukemia Research Fund, and Michael and Judy Thomas. C.R.L. is a recipient of a National Institutes of Health T32 Award in Oncology Training Fellowship at The Ohio State University Comprehensive Cancer Center (T32-CA009338).

Authorship

Contribution: E.M.M., C.R.L., T.C., N.M., and J.C.B. designed and performed research, analyzed data, and wrote the paper; A.C., W.E.C., and C.M.C. designed and performed research, analyzed the data, and approved the final version of the paper; X.M. provided statistical analysis, reviewed drafts, and approved the final version of the paper; C.E.C. and E.H. designed research, reviewed drafts, and approved the final version of the paper; S.T., J.B., B.K.H., and R.W. performed research, reviewed drafts, and approved the final version of the paper; and J.W., K.A.R., L.A.A., and F.T.A. provided patient samples, reviewed drafts, and approved the final version of the paper.

Conflict-of-interest disclosure: K.A.R. has received research funding from Genentech. F.T.A. has received research funding from Innate Pharma and provided consulting services to Gilead Sciences, Pharmacyclics, Inc., and Novartis Oncology. L.A.A. has received research funding from Sanofi. J.W. has received research funding from Acerta Pharma, Karyopharm Therapeutics, and MorphoSys AG. J.C.B. has received research funding from Acerta Pharma, Pharmacyclics, Inc., and Genentech. The remaining authors declare no competing financial interests.

ORCID profile: F.T.A., 0000-0003-1813-9812.

Correspondence: Natarajan Muthusamy, Division of Hematology, Department of Internal Medicine, College of Medicine, The Ohio State University, 400 W 12th Ave, Wiseman Hall, Room 455 Columbus, OH 43210; e-mail: raj.muthusamy@osumc.edu; and John C. Byrd, Division of Hematology, Department of Internal Medicine, College of Medicine, The Ohio State University, 400 W 12th Ave, Wiseman Hall, Room 455, Columbus, OH 43210; e-mail: john.byrd@osumc.edu.

References

1. Hallek M, Fischer K, Fingerle-Rowson G, et al; German Chronic Lymphocytic Leukaemia Study Group. Addition of rituximab to fludarabine and cyclophosphamide in patients with chronic lymphocytic leukaemia: a randomised, open-label, phase 3 trial. *Lancet*. 2010;376(9747):1164-1174.
2. Thompson PA, Tam CS, O'Brien SM, et al. Fludarabine, cyclophosphamide, and rituximab treatment achieves long-term disease-free survival in IGHV-mutated chronic lymphocytic leukemia. *Blood*. 2016;127(3):303-309.
3. Byrd JC, Rai K, Peterson BL, et al. Addition of rituximab to fludarabine may prolong progression-free survival and overall survival in patients with previously untreated chronic lymphocytic leukemia: an updated retrospective comparative analysis of CALGB 9712 and CALGB 9011. *Blood*. 2005;105(1):49-53.
4. Golay J, Da Roit F, Bologna L, et al. Glycoengineered CD20 antibody obinutuzumab activates neutrophils and mediates phagocytosis through CD16B more efficiently than rituximab. *Blood*. 2013;122(20):3482-3491.
5. Rafiq S, Butchar JP, Cheney C, et al. Comparative assessment of clinically utilized CD20-directed antibodies in chronic lymphocytic leukemia cells reveals divergent NK cell, monocyte, and macrophage properties. *J Immunol*. 2013;190(6):2702-2711.
6. Goede V, Fischer K, Busch R, et al. Obinutuzumab plus chlorambucil in patients with CLL and coexisting conditions. *N Engl J Med*. 2014;370(12):1101-1110.
7. Herman SE, Gordon AL, Hertlein E, et al. Bruton tyrosine kinase represents a promising therapeutic target for treatment of chronic lymphocytic leukemia and is effectively targeted by PCI-32765. *Blood*. 2011;117(23):6287-6296.
8. Ponader S, Chen SS, Buggy JJ, et al. The Bruton tyrosine kinase inhibitor PCI-32765 thwarts chronic lymphocytic leukemia cell survival and tissue homing in vitro and in vivo. *Blood*. 2012;119(5):1182-1189.
9. Byrd JC, Furman RR, Coutre SE, et al. Targeting BTK with ibrutinib in relapsed chronic lymphocytic leukemia. *N Engl J Med*. 2013;369(1):32-42.
10. Burger JA, Styles L, Kipps TJ. Ibrutinib for chronic lymphocytic leukemia. *N Engl J Med*. 2016;374(16):1594-1595.
11. O'Brien S, Furman RR, Coutre S, et al. Single-agent ibrutinib in treatment-naïve and relapsed/refractory chronic lymphocytic leukemia: a 5-year experience. *Blood*. 2018;131(17):1910-1919.
12. Ahn IE, Farooqui MZH, Tian X, et al. Depth and durability of response to ibrutinib in CLL: 5-year follow-up of a phase 2 study. *Blood*. 2018;131(21):2357-2366.
13. Maddocks KJ, Ruppert AS, Lozanski G, et al. Etiology of ibrutinib therapy discontinuation and outcomes in patients with chronic lymphocytic leukemia. *JAMA Oncol*. 2015;1(1):80-87.
14. Woyach JA, Ruppert AS, Guinn D, et al. BTK^{C481S}-mediated resistance to ibrutinib in chronic lymphocytic leukemia. *J Clin Oncol*. 2017;35(13):1437-1443.
15. Woyach JA, Furman RR, Liu TM, et al. Resistance mechanisms for the Bruton's tyrosine kinase inhibitor ibrutinib. *N Engl J Med*. 2014;370(24):2286-2294.

16. Burger JA, Keating MJ, Wierda WG, et al. Safety and activity of ibrutinib plus rituximab for patients with high-risk chronic lymphocytic leukaemia: a single-arm, phase 2 study. *Lancet Oncol*. 2014;15(10):1090-1099.

17. Bojarczuk K, Siernicka M, Dwojak M, et al. B-cell receptor pathway inhibitors affect CD20 levels and impair antitumor activity of anti-CD20 monoclonal antibodies. *Leukemia*. 2014;28(5):1163-1167.

18. Skarzynski M, Niemann CU, Lee YS, et al. Interactions between ibrutinib and anti-CD20 antibodies: competing effects on the outcome of combination therapy. *Clin Cancer Res*. 2016;22(1):86-95.

19. Kohrt HE, Sagiv-Barfi I, Rafiq S, et al. Ibrutinib antagonizes rituximab-dependent NK cell-mediated cytotoxicity. *Blood*. 2014;123(12):1957-1960.

20. Schneider P, MacKay F, Steiner V, et al. BAFF, a novel ligand of the tumor necrosis factor family, stimulates B cell growth. *J Exp Med*. 1999;189(11): 1747-1756.

21. Moore PA, Belvedere O, Orr A, et al. BLyS: member of the tumor necrosis factor family and B lymphocyte stimulator. *Science*. 1999;285(5425):260-263.

22. Yan M, Brady JR, Chan B, et al. Identification of a novel receptor for B lymphocyte stimulator that is mutated in a mouse strain with severe B cell deficiency. *Curr Biol*. 2001;11(19):1547-1552.

23. Thompson JS, Bixler SA, Qian F, et al. BAFF-R, a newly identified TNF receptor that specifically interacts with BAFF. *Science*. 2001;293(5537): 2108-2111.

24. Rodig SJ, Shahsafaei A, Li B, Mackay CR, Dorfman DM. BAFF-R, the major B cell-activating factor receptor, is expressed on most mature B cells and B-cell lymphoproliferative disorders. *Hum Pathol*. 2005;36(10):1113-1119.

25. Gardam S, Sierro F, Basten A, Mackay F, Brink R. TRAF2 and TRAF3 signal adapters act cooperatively to control the maturation and survival signals delivered to B cells by the BAFF receptor. *Immunity*. 2008;28(3):391-401.

26. Claudio E, Brown K, Park S, Wang H, Siebenlist U. BAFF-induced NEMO-independent processing of NF-kappa B2 in maturing B cells. *Nat Immunol*. 2002;3(10):958-965.

27. Kayagaki N, Yan M, Seshasayee D, et al. BAFF/BLyS receptor 3 binds the B cell survival factor BAFF ligand through a discrete surface loop and promotes processing of NF-kappaB2. *Immunity*. 2002;17(4):515-524.

28. Burger JA. Targeting the microenvironment in chronic lymphocytic leukemia is changing the therapeutic landscape. *Curr Opin Oncol*. 2012;24(6): 643-649.

29. Cols M, Barra CM, He B, et al. Stromal endothelial cells establish a bidirectional crosstalk with chronic lymphocytic leukemia cells through the TNF-related factors BAFF, APRIL, and CD40L. *J Immunol*. 2012;188(12):6071-6083.

30. Nishio M, Endo T, Tsukada N, et al. Nurselike cells express BAFF and APRIL, which can promote survival of chronic lymphocytic leukemia cells via a paracrine pathway distinct from that of SDF-1alpha. *Blood*. 2005;106(3):1012-1020.

31. Johnson AJ, Lucas DM, Muthusamy N, et al. Characterization of the TCL-1 transgenic mouse as a preclinical drug development tool for human chronic lymphocytic leukemia. *Blood*. 2006;108(4):1334-1338.

32. Enzler T, Kater AP, Zhang W, et al. Chronic lymphocytic leukemia of Emu-TCL1 transgenic mice undergoes rapid cell turnover that can be offset by extrinsic CD257 to accelerate disease progression. *Blood*. 2009;114(20):4469-4476.

33. Zhao X, Lwin T, Silva A, et al. Unification of de novo and acquired ibrutinib resistance in mantle cell lymphoma. *Nat Commun*. 2017;8:14920.

34. Qin H, Wei G, Sakamaki I, et al. Novel BAFF-receptor antibody to natively folded recombinant protein eliminates drug-resistant human B-cell malignancies in vivo. *Clin Cancer Res*. 2018;24(5):1114-1123.

35. Parameswaran R, Lim M, Fei F, et al. Effector-mediated eradication of precursor B acute lymphoblastic leukemia with a novel Fc-engineered monoclonal antibody targeting the BAFF-R. *Mol Cancer Ther*. 2014;13(6):1567-1577.

36. Hallek M, Cheson BD, Catovsky D, et al; International Workshop on Chronic Lymphocytic Leukemia. Guidelines for the diagnosis and treatment of chronic lymphocytic leukemia: a report from the International Workshop on Chronic Lymphocytic Leukemia updating the National Cancer Institute-Working Group 1996 guidelines. *Blood*. 2008;111(12):5446-5456.

37. Hertlein E, Beckwith KA, Lozanski G, et al. Characterization of a new chronic lymphocytic leukemia cell line for mechanistic in vitro and in vivo studies relevant to disease. *PLoS One*. 2013;8(10):e76607.

38. Bichi R, Shinton SA, Martin ES, et al. Human chronic lymphocytic leukemia modeled in mouse by targeted TCL1 expression. *Proc Natl Acad Sci U S A*. 2002;99(10):6955-6960.

39. Overdijk MB, Jansen JH, Nederend M, et al. The therapeutic CD38 monoclonal antibody daratumumab induces programmed cell death via Fcγ receptor-mediated cross-linking. *J Immunol*. 2016;197(3):807-813.

40. Verbeke G, Molenberghs G. Linear Mixed Models for Longitudinal Data. New York, NY: Springer-Verlag; 2009

41. Hsu J. Multiple Comparisons: Theory and Methods. *Boca Raton, FL*: CRC Press; 1996

42. Novak AJ, Grote DM, Stenson M, et al. Expression of BLyS and its receptors in B-cell non-Hodgkin lymphoma: correlation with disease activity and patient outcome. *Blood*. 2004;104(8):2247-2253.

43. He B, Chadburn A, Jou E, Schattner EJ, Knowles DM, Cerutti A. Lymphoma B cells evade apoptosis through the TNF family members BAFF/BLyS and APRIL. *J Immunol*. 2004;172(5):3268-3279.

44. Endo T, Nishio M, Enzler T, et al. BAFF and APRIL support chronic lymphocytic leukemia B-cell survival through activation of the canonical NF-kappaB pathway. *Blood*. 2007;109(2):703-710.

45. Cooper S, Bakal C. Accelerating live single-cell signalling studies. *Trends Biotechnol*. 2017;35(5):422-433.

46. Irish JM, Kotecha N, Nolan GP. Mapping normal and cancer cell signalling networks: towards single-cell proteomics. *Nat Rev Cancer*. 2006;6(2):146-155.

47. Shinners NP, Carlesso G, Castro I, et al. Bruton's tyrosine kinase mediates NF-kappa B activation and B cell survival by B cell-activating factor receptor of the TNF-R family [published correction appears in *J Immunol*. 2007;179(9):6369]. *J Immunol*. 2007;179(6):3872-3880.

48. De Maria A, Bozzano F, Cantoni C, Moretta L. Revisiting human natural killer cell subset function revealed cytolytic CD56(dim)CD16+ NK cells as rapid producers of abundant IFN-γ on activation. *Proc Natl Acad Sci USA*. 2011;108(2):728-732.

49. Wang R, Jaw JJ, Stutzman NC, Zou Z, Sun PD. Natural killer cell-produced IFN-γ and TNF-α induce target cell cytolysis through up-regulation of ICAM-1. *J Leukoc Biol*. 2012;91(2):299-309.

50. de Haij S, Jansen JH, Boross P, et al. In vivo cytotoxicity of type I CD20 antibodies critically depends on Fc receptor ITAM signaling. *Cancer Res*. 2010;70(8):3209-3217.

51. Long M, Beckwith K, Do P, et al. Ibrutinib treatment improves T cell number and function in CLL patients. *J Clin Invest*. 2017;127(8):3052-3064.